

# Spin fluctuation driven enhancement of thermopower near the quantum critical point in $\text{Ba}(\text{Fe}_{1-x}\text{Co}_x)_2\text{As}_2$

S. Arsenijević,<sup>1</sup> H. Hodovanets,<sup>2</sup> R. Gaál,<sup>1</sup> L. Forró,<sup>1</sup> S. L. Bud'ko,<sup>2</sup> and P. C. Canfield<sup>2</sup>

<sup>1</sup>*Institute of Condensed Matter Physics, Swiss Federal Institute of Technology, EPFL, CH-1015 Lausanne, Switzerland*

<sup>2</sup>*Ames Laboratory, US DOE, and Department of Physics and Astronomy, Iowa State University, Ames, Iowa 50011, USA*

We demonstrate that the thermopower ( $S$ ) can be used to probe the spin fluctuations (SF) in the proximity to the quantum critical point (QCP) in Fe-based superconductors. The sensitivity of  $S$  to the entropy of charge carriers allows us to observe an increase of  $S/T$  in  $\text{Ba}(\text{Fe}_{1-x}\text{Co}_x)_2\text{As}_2$  close to the spin-density-wave (SDW) QCP. This behavior is due to the coupling of low-energy conduction electrons to two-dimensional SF, similar to the heavy-fermion systems. The low-temperature enhancement of  $S/T$  in the doping range  $0.02 < x < 0.1$  is bordered by the two Lifshitz transitions, and it corresponds to the superconducting doping region, where similarity between the electron and nonreconstructed hole pockets exists. The maximal  $S/T$  is observed in the proximity of commensurate-to-incommensurate SDW transition, for critical  $x_c \approx 0.06$ , close to the highest superconducting  $T_c$ . This analysis indicates that the low- $T$  thermopower is influenced by the critical spin fluctuations which are important for the superconducting mechanism.

The physical properties of matter in the vicinity of a quantum critical point (QCP) have been in the focus of interest since the discovery of unconventional superconductivity [1] and heavy-fermion systems [2]. The discovery of superconductivity (SC) in Fe-based materials (FeSC) and the presence of a spin-density-wave (SDW) state motivated discussions about the interplay of magnetism, structure and superconductivity simultaneous with the existence of a QCP in the phase diagram of FeSC [3]. The structural, tetragonal-to-orthorhombic, transition is coupled to the paramagnetic-to-antiferromagnetic transition [4]. This behavior can be realized through nematic order which emerges from the coexistence of magnetic fluctuations and frustration [5–7]. It explains the proximity in temperature of the structural ( $T_S$ ) and magnetic ( $T_{SDW}$ ) transitions throughout the phase diagram of doped iron-pnictides [8]. The observed anisotropy of the in-plane resistivity is in agreement with the nematic scenario of anisotropic electronic states originating from the scattering by impurities and critical spin fluctuations (SF) [6, 9, 10]. The magnetic fluctuations are important because it is believed they are responsible for the SC pairing [11].

The thermoelectric power ( $S$ ) is sensitive to the derivative of density of electronic states and the change of the relaxation time close to the Fermi surface (FS). It can be interpreted as the entropy per charge carrier [12].  $S$  can be used to detect deviations from the Landau Fermi-liquid (FL) picture, *i.e.* in heavy-fermion compounds. There, the enhanced scattering by critical SF close to the antiferromagnetic (AF) quantum critical point leads to an increase of electronic entropy and, consequently, to increases of thermopower and electronic specific heat ( $C_e$ ) [13]. The increase of entropy and  $C_e$  upon entering the nematic phase in the vicinity of the quantum critical phase was shown in the example of  $\text{Sr}_3\text{Ru}_2\text{O}_7$  [14]. In this paper, we observe quantum critical behavior by thermopower in the phase diagram of the prototypical

Fe-based superconductor  $\text{Ba}(\text{Fe}_{1-x}\text{Co}_x)_2\text{As}_2$  (BFCA).

The variation of thermopower  $S/T$  have been used to characterize the nature of the QCP in non-Fermi-liquid (NFL) heavy-fermion compounds [15]. In the case of a spin-density-wave criticality, the  $S/T$  is roughly symmetric around QCP. Also, it was shown that  $S/T$  near the magnetic quantum critical point has a similar variation as  $C_e/T$  [13]. The low energy quasi-2D spin fluctuations with a 2D ordering wave vector and a 3D Fermi surface, lead to hot regions on the FS. The electrons are strongly renormalized in these regions because of the enhanced scattering on nearly critical SF. This leads to the following expression for the specific heat or entropy per particle:  $C_e/N \propto T(1/\epsilon_F \omega_S) \ln(\omega_S/\delta)$ . Here,  $\omega_S$  is the energy of the spin fluctuations,  $\epsilon_F$  is the Fermi energy,  $\delta$  is the mass of SF and it measures the deviation from the QCP. The logarithmic  $T$ -dependence of specific heat is different from the Fermi-liquid behavior in which  $C_e \propto T$ . Analogously, the expression for thermopower based on critical 2D-SF is  $S \propto T(1/\epsilon_F \omega_S) \ln(\omega_S/\delta)$  [13]. One can write  $\delta$  as  $\delta = \Gamma(p - p_c) + T$ , where  $\Gamma$  is an energy parameter and  $p$  is an experimental parameter (doping, pressure or magnetic field) that can be tuned to the critical value  $p_c$ . This means that the QCP can be approached by changing the temperature or other parameters in the system. In the former case, when  $T > \Gamma(p - p_c)$ ,  $S$  in the proximity to QCP has a dependence  $S/T \propto \ln(1/T)$ , qualitatively different from the FL behavior  $S/T \propto \text{const.}$  [13].

The NFL divergent behavior of  $S/T$  close to antiferromagnetic SDW QCP is observed in several unconventional superconductors, among others: heavy-fermions  $\text{Ce}_2\text{PdIn}_8$  [16], cuprate high- $T_c$  superconductor  $\text{La}_{1.6-x}\text{Nd}_{0.4}\text{Sr}_x\text{CuO}_4$  [17], hole-doped Fe-pnictides  $\text{Ba}_{1-x}\text{K}_x\text{Fe}_2\text{As}_2$ ,  $\text{Sr}_{1-x}\text{K}_x\text{Fe}_2\text{As}_2$  [18, 19], and  $\text{Eu}_{1-x}\text{K}_x\text{Fe}_2\text{As}_2$  [20]. The difference between these compounds is the energy defined by  $T$  below which critical behavior is observed and SC emerges, which is smaller in heavy-fermion and larger in high- $T_c$  SC. Another sign

of quantum critical behavior is the  $T$ -linear resistivity  $\rho(T)$  driven by anomalous scattering on spin fluctuations, for the critical value of a tuning parameter, which was reported in all of the aforementioned compounds [17–19, 21]. Also, the critical behavior of  $\rho(T)$  corresponds to the highest SC  $T_c$ , thus supporting the SF driven SC scenario [1]. The highest energy range of criticality is observed in  $\text{La}_{2-x}\text{Sr}_x\text{CuO}_4$  cuprates where the linear  $T$ -dependence of  $\rho$  extends up to 1100 K [22]. In both cuprates and Fe-pnictides, this anomalous behavior is observed only in a narrow doping range, for a critical value of the parameter [18, 23, 24].

Here we focus on the  $S/T$  in the low- $T$  region that shows anomalous behavior in electron-doped BFCA. SDW long-range AF order at  $T_{SDW}$  is defined by a commensurate propagation vector  $(\pi, \pi)$  which is the nesting vector between the hole and electron pockets on the Fermi surface [25]. The  $T_{SDW}$  occurs lower than  $T_S$  transition [26] and in the SDW phase the FS is reconstructed [27]. With doping, the structural/SDW transitions are suppressed and increasingly separated, and the FS undergoes a Lifshitz transition above  $x \approx 0.02$  [27, 28]. It is a topological change of the FS, and the first one occurs when the reconstructed hole-pocket disappears below the Fermi level giving way to the electron-pocket at the Brillouin zone X-corner (LT1). A similarity in size and shape of this electron X-pocket and the hole  $\Gamma$ -pocket in the zone center exists in the  $0.02 < x < 0.1$  range [28]. This feature enhances interband scattering which is important for the superconducting pairing [25, 29–31]. The low-energy spin resonance observed in the SC phase by inelastic neutron scattering at the same nesting vector supports the picture of a SC pairing mechanism mediated by spin fluctuations [32]. Also, nuclear magnetic resonance links the strength of AF SF and SC  $T_c$ , when the SDW order is almost suppressed [33]. In the same region, for  $x \approx 6\%$ , the magnetic wave vector becomes incommensurate with the lattice periodicity [34].

The tightly spaced doping in  $\text{Ba}(\text{Fe}_{1-x}\text{Co}_x)_2\text{As}_2$  single crystals allows us to precisely map the whole  $S/T$  phase diagram [35, 36]. Thus, we can study the evolution of  $S$  as the system undergoes several Lifshitz transitions [28]. They were observed by angle-resolved photoemission spectroscopy (ARPES) [27] and the change in thermopower and Hall effect [36]. Between the first two Lifshitz transitions, interband scattering is responsible for the AF SF and thermopower is sensitive to them. Therefore, we can probe the phase diagram of Fe-pnictides, in order to search for the signatures of spin fluctuation driven quantum criticality in  $S/T$ .

The temperature dependence of  $|S|/T$  vs.  $\ln T$  for the whole phase diagram is presented in Fig. 1. We separated the data into three groups which show characteristic  $T$ -dependence: (Fig. 1a) for  $x = 0-0.025$   $S/T$  undergoes an abrupt change at  $T_S$  followed by the Fermi surface reconstruction [27]. The reconstructed hole Dirac-like band in

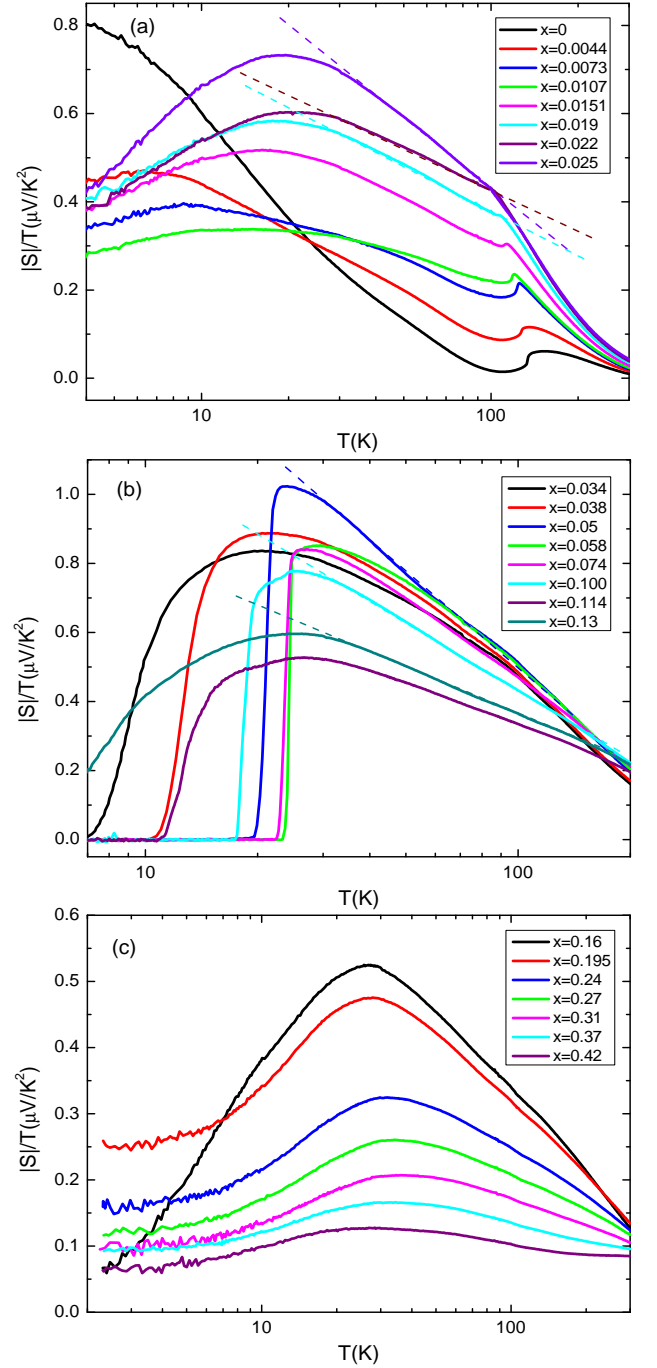


FIG. 1. The behavior of  $S/T$  vs.  $\ln T$  in three doping regimes: (a) SDW phase in which the Fermi surface is reconstructed, (b) superconducting, (c) toward the Fermi-liquid at high  $x$ . Dotted lines emphasize linearity on a log- $T$  scale. Thermopower data are taken from [35] and [36].

the SDW state was predicted [37] and observed [38] and it induces a positive contribution to the otherwise small and compensated thermopower of  $\text{BaFe}_2\text{As}_2$  [39]. This contribution to  $S$  is  $T$ -dependent [40] and it is suppressed with doping [35]. Its decrease is responsible for the increase of  $|S|/T$  with lowering temperature in the low-doping

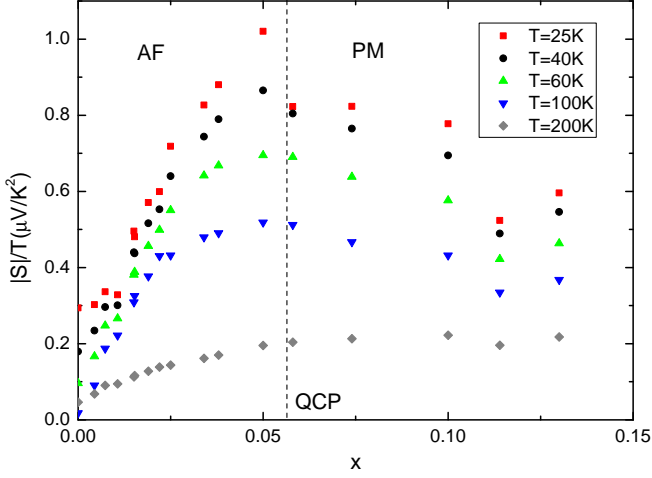


FIG. 2.  $S/T$  diverges when approaching the QCP around  $x_c \approx 0.056$ , and the parameter  $\delta$  (the mass of SF) is decreasing. The same effect is achieved by decreasing  $\delta$  with lowering temperature. In the AF phase the drop is more abrupt, similar to theoretical calculation [15].

regime. As we approach the Lifshitz transition at  $x \approx 0.025$  the quantum critical behavior  $S/T \propto \ln(1/T)$  can be observed in a limited  $T$ -range [30-100K]. (Fig. 1b) The Lifshitz transition LT1 is crossed and the  $S/T$  diverges linearly on the  $\log T$ -scale with lowering  $T$ . With doping, the slope of  $S/T$  increases up to  $x = 0.05$  and then decreases. Taking into account the expressions for  $S$  in the quantum critical regime  $S/T \propto \ln(\omega_S/\delta)$  and mass of spin fluctuation  $\delta = \Gamma(p - p_c) + T$ , we can explain the log-increase of  $S$  with lowering  $T$  and decreasing SF mass  $\delta$ . When  $T < \Gamma(p - p_c)$ ,  $S$  starts to saturate depending on the value of parameter  $p$ , in this case doping  $x$ . Above the second Lifshitz transition (LT2) at  $x \approx 0.11$  the cylindrical hole band changes to ellipsoid [28], which reduces the nesting and  $S/T$ . (Fig. 1c) As the superconductivity is suppressed above  $x = 0.14$ , the slope of  $S(T)/T$  continues to decrease. This can be explained with continuous increase of  $\delta$  that results in smaller  $S$ . The system undergoes a third Lifshitz transition (LT3) around  $x \approx 0.2$ , above which the hole band is suppressed below the Fermi level. Above that doping, low- $T$   $S/T$  saturates as the system makes a cross-over from a quantum critical NFL to the Fermi-liquid-like ( $S/T \propto \text{const.}$ ) state.

If we analyze the doping-dependent behavior of  $S$  at fixed temperatures, we observe that for the critical value of  $x_c \approx 0.06$ , the  $S/T$  attains its highest value and has a broad maximum centered at the QCP (Fig. 2). The  $x$ -dependence comes from the change of the spin fluctuation mass  $\delta$  in the expression for  $S$ . This behavior is in agreement with the theoretical calculations, which show that  $S/T$  diverges in the proximity to the QCP in SDW systems [13, 15]. As predicted, the rate of change of

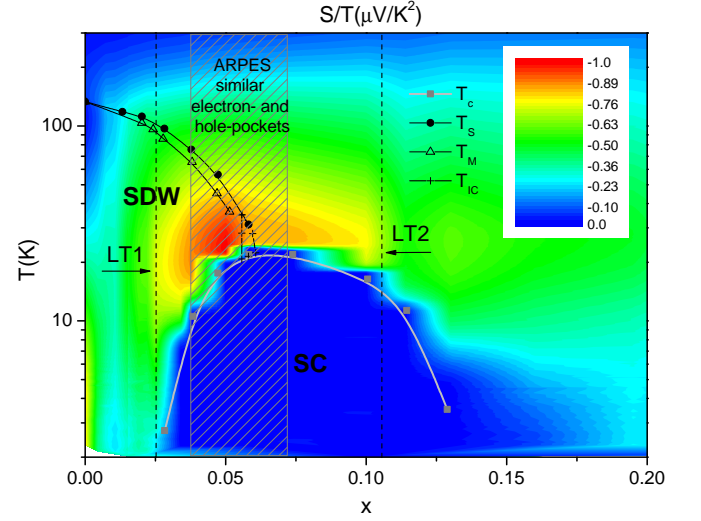


FIG. 3. Contour plot of  $S/T$  as a function of  $\log T$  and doping  $x$ , shows a low- $T$  increase due to spin fluctuations in the region of similar non-reconstructed electron X-pocket and hole- $\Gamma$  pocket, in the  $x$ -range between the first (LT1) and second (LT2) Lifshitz transition. The temperature of the superconducting ( $T_c$ ), structural ( $T_s$ ), and antiferromagnetic ( $T_m$ ) transition are taken from ref. [45, 46]. The region of the incommensurate-SDW is indicated by  $T_{IC}$  [34]. The  $x$ -levels that correspond to the Lifshitz transitions are taken from ref. [28] and the similarity between the electron- and hole-pocket was reported in ref. [27].

$S/T(x)$  in the AF phase is more pronounced than in the paramagnetic phase, because of the reduction of entropy in the AF ordered phase. In the overdoped case ( $x > 0.2$ ), the hole band is suppressed below the Fermi level and the bandwidth of the electron band is much larger, in agreement with the Fermi-liquid dependence seen in resistivity ( $\rho \propto T^2$ ) [41, 42] and thermopower (Fig. 1c). On the other hand, the region closer to QCP is characterized by  $T$ -linear NFL  $\rho$ , in analogy with cuprates and Bechgaard salts [42]. A similar cross-over was observed in a heavy-fermion compound  $\text{YbRh}_2(\text{Si}_{1-x}\text{Ge}_x)_2$ , at the transition from the magnetic field-induced FL ( $C_e/T \propto \text{const.}$ ) and the NFL state [43]. In the same compound,  $S/T$  was found to diverge similarly to  $C_e/T$  in the NFL state, indicating a large entropy of charge carriers [44].

A more suggestive representation of the  $S/T$  data presented in Fig. 1 is the contour plot of  $S/T$  as a function of doping and  $\log T$  in Fig. 3.  $S/T$  maps a 'hot' region above the SC dome, bordered by the two Lifshitz transitions, LT1 and LT2, with a dome-like distribution of intensity. In this doping region ( $x = 0.025$ -0.1) the size of the electron X- and hole  $\Gamma$ -pocket is similar [27]. The peak of intensity is close to  $x = 0.05$ , where the QCP is approached, close to the reported incommensurate spin-density-wave (IC-SDW) region, that was observed by neutron diffraction in the doping range between  $0.056 < x < 0.06$  [34]. The doping-induced

suppression of the structural and magnetic transitions leads to the weakening of a nesting-driven SDW order which results in an enhancement of the spin fluctuations in the region marked by red color in the Fig. 3. It is the same region of the phase diagram where the back-bending of the separate SDW and structural tetragonal-to-orthorhombic transition occurs below SC  $T_c$  [8, 47]. The observed competition between the superconductivity and magnetism/orthorhombicity is explained by the magnetoelastic coupling and the closely related nematic order. The nematic fluctuations above  $T_S$  are coupled to the lattice in the normal state, which induces the concomitant structural and nematic transition followed by the magnetic transition at lower temperature [6, 48].

The divergence of  $S/T$  at  $x_c$  from the both higher and lower doping side is reminiscent of the behavior observed in  $\text{Sr}_3\text{Ru}_2\text{O}_7$ , in which magnetic field was used as a tuning parameter to approach the QCP [14]. A jump in magnitude observed there in two thermodynamic variables, entropy and specific heat, was ascribed to the formation of a spin nematic phase of electronic fluid with broken rotational symmetry. This phase was previously detected as a region with highly anisotropic magnetoresistivity [49]. The behavior of our system is analogous with this: increase of  $S/T$  in the  $x-T$  phase diagram matches the region of increased in-plane resistivity anisotropy observed in ref. [9]. These two phase diagrams indicate a formation of a novel quantum phase, the electronic nematic phase, in the vicinity of QCP in Fe-based superconductor, in agreement with the nematic order scenario [6].

There are many complex systems in which IC-SDW, nematic stripe order, high thermopower and superconductivity are reported to coexist. For example, spin entropy was suggested to be responsible for the enhanced  $S$  in  $\text{Na}_x\text{Co}_2\text{O}_4$  [50] and superconducting  $\text{Na}_x\text{Co}_2\text{O}_4 \cdot \gamma\text{H}_2\text{O}$  [51, 52]. One can argue that this can be generalized to other complex transition-metal oxides, including the high- $T_c$  cuprates [53, 54]. Essentially the same behavior, compared to FeSC, was observed by the application of pressure or chemical doping to the itinerant antiferromagnet Cr [55, 56]. There, the nesting-driven SDW transition is suppressed with the change of external parameters, resulting in quantum critical behavior at low- $T$ . Unlike FeSC, the SC  $T_c$  is never high in Cr alloys because of the lack of sufficiently attractive electron-electron interaction necessary for the Cooper pair formation [56].

Strong evidence for the connection between SC and the observed quantum criticality is the correlation between the doping dependence of  $T_c$ ,  $S/T$  and the specific heat jump ( $\Delta C_p/T_c$ ) at the SC  $T_c$  which changes by a factor of  $\sim 10$  across the SC dome [57].  $\Delta C_p/T_c$  vs.  $T_c$  data for several FeSC can be scaled linearly to a single log-log plot over an order of magnitude in  $T_c$ . We propose that spin entropy plays a crucial role in the maximum of  $\Delta C_p/T_c$ , and that the highest entropy comes from the IC-SDW for  $x \sim 0.05$ . The striking similarity between the doping

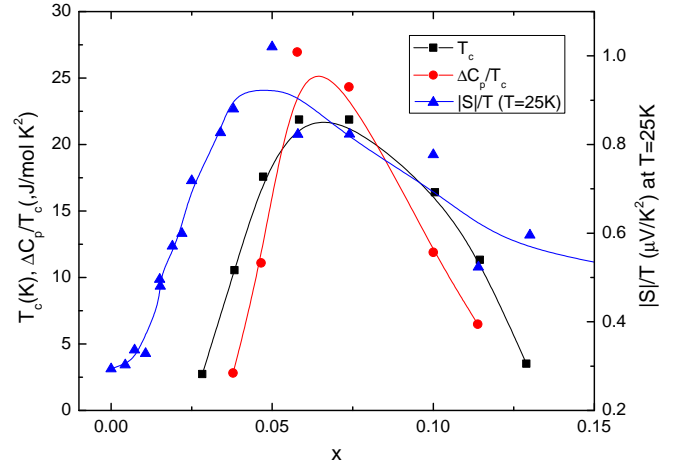


FIG. 4. Superconducting transition  $T_c$ , specific heat jump  $\Delta C_p/T_c$ , and the entropy (thermopower,  $S/T$ ) at  $T=25\text{K}$  as a function of concentration  $x$  in  $\text{Ba}(\text{Fe}_{1-x}\text{Co}_x)_2\text{As}_2$ . Specific heat data are from ref. [57]. Lines serve as a guide to the eye.

dependence of SC  $T_c$ ,  $\Delta C_p/T_c$ , and  $S/T$  is presented in the Fig. 4. The proportionality of the  $T_c$  and the strength of spin fluctuations observed in  $S/T$  support the picture of SF mediated superconductivity. The SF determine the energy scale which results in the dome-like behavior in  $T_c$ ,  $\Delta C_p/T_c$ , and  $S/T$ . This can also be observed in the proximity of thermopower intensity peak to the maximal  $T_c$  in Fig. 3.

The spin fluctuations are also proportional to the resonance observed in the inelastic neutron scattering at the interband scattering vector  $(\pi, \pi)$  [32]. Also, a recent, more detailed neutron study on FeSC proved that the commensuration in the spin excitation spectrum and the so-called hour-glass dispersion forms well above SC  $T_c$  [58]. The same technique detected spin excitations in the SC hole-doped  $\text{Ba}_{1-x}\text{K}_x\text{Fe}_2\text{As}_2$ , where the correlation between the Fermi surface nesting, SF energy and SC  $T_c$  is observed [59]. The additional correlation with the critical fluctuations observed by  $S/T$  in the same compound supports the argument of this paper [19]. Nernst effect study on a similar compound  $\text{Eu}(\text{Fe}_{1-x}\text{Co}_x)_2\text{As}_2$  showed the existence of an anomalous contribution that peaks above  $T_c$  (around 40K) in the sample where SDW and SC coexist [60]. The authors there associated this contribution with the Fermi-surface reconstruction caused by spin fluctuations. Future Nernst effect measurements in BFCA compound can bring useful information concerning the existence of SF above  $T_c$ .

We observe a signature of quantum critical behavior in the  $T$ -dependence of thermopower of the Fe-based superconductor  $\text{Ba}(\text{Fe}_{1-x}\text{Co}_x)_2\text{As}_2$ . We ascribe the increase seen in  $S/T(T, x)$  around critical doping  $x_c$  to spin fluctuation close to the QCP. The origin of it are the SDW driven critical SF that are enhanced at low- $T$  for  $0.02 < x < 0.1$ , between the two Lifshitz transitions, where

the electron and hole pockets are well nested. The smallest mass of SF and the largest  $S/T$  at low- $T$  correspond to  $x_c \approx 0.05$ , close to the reported IC-SDW region. The quantum critical behavior that we observe in  $S/T$  confirms the behavior found in  $\rho$  and its anisotropy. Thus, the enhancement of thermopower and consequently, entropy of electron system, in Fe-pnictides can be related to SF, which exist above the SC  $T_c$ . Their strength is proportional to the  $T_c$ , which supports the picture of spin fluctuation mediated superconductivity.

Work performed at EPFL was supported by the Swiss NSF and by the MaNEP NCCR. Part of this work was performed at the Ames Laboratory and supported by the U.S. Department of Energy, Office of Basic Energy Science, Division of Materials Sciences and Engineering. Ames Laboratory is operated for the U.S. Department of Energy by Iowa State University under Contract No. DE-AC02-07CH11358.

- 
- [1] L. Taillefer, *Annu. Rev. Cond. Matter Phys.* **1**, 51 (2010).
  - [2] P. Gegenwart, Q. Si and F. Steglich, *Nature Physics* **4**, 186 (2008).
  - [3] J. Dai *et al.*, *Proc. Natl. Acad. Sci.* **106**, 4118 (2009).
  - [4] Q. Huang *et al.*, *Phys. Rev. Lett.* **101**, 257003 (2008).
  - [5] C. Xu, M. Müller and S. Sachdev, *Phys. Rev. B* **78**, 020501 (2008).
  - [6] R. M. Fernandes, E. Abrahams and J. Schmalian, *Phys. Rev. Lett.* **107**, 217002 (2011).
  - [7] C. Fang *et al.*, *Phys. Rev. B* **77**, 224509 (2008).
  - [8] S. Nandi *et al.*, *Phys. Rev. Lett.* **104**, 057006 (2010).
  - [9] J.-H. Chu *et al.*, *Science* **329**, 824 (2010).
  - [10] M. A. Tanatar *et al.*, *Phys. Rev. B* **81**, 184508 (2010).
  - [11] P. Monthoux *et al.*, *Nature* **450**, 1177 (2007).
  - [12] P. M. Chaikin and G. Beni, *Phys. Rev. B* **13**, 647 (1976).
  - [13] I. Paul and G. Kotliar, *Phys. Rev. B* **64**, 184414 (2001).
  - [14] A. W. Rost *et al.*, *Science* **325**, 1360 (2009).
  - [15] K.-S. Kim and C. Pépin, *Phys. Rev. B* **81**, 205108 (2010).
  - [16] M. Matusiak *et al.*, *Phys. Rev. B* **84**, 115110 (2011).
  - [17] R. Daou *et al.*, *Phys. Rev. B* **79**, 180505 (2009).
  - [18] M. Gooch *et al.*, *Phys. Rev. B* **79**, 104504 (2009).
  - [19] M. Gooch *et al.*, *J. of Appl. Phys.* **107**, 09E145 (2010).
  - [20] J. Maiwald *et al.*, *Phys. Rev. B* **85**, 024511 (2012).
  - [21] J. K. Dong *et al.*, *Phys. Rev. X* **1**, 011010 (2011).
  - [22] M. Gurvitch and A. T. Fiory, *Phys. Rev. Lett.* **59**, 1337 (1987).
  - [23] Y. Ando *et al.*, *Phys. Rev. Lett.* **93**, 267001 (2004).
  - [24] S. Kasahara *et al.*, *Phys. Rev. B* **81**, 184519 (2010).
  - [25] K. Terashima *et al.*, *Proc. Natl. Acad. Sci.* **106**, 7330 (2009).
  - [26] M. G. Kim *et al.*, *Phys. Rev. B* **83**, 134522, (2011).
  - [27] C. Liu *et al.*, *Nature Physics* **6**, 419-423 (2010).
  - [28] C. Liu *et al.*, *Phys. Rev. B* **84**, 020509 (2011).
  - [29] I. I. Mazin *et al.*, *Phys. Rev. Lett.* **101**, 057003 (2008).
  - [30] K. Kuroki *et al.*, *Phys. Rev. Lett.* **101**, 087004 (2008).
  - [31] M. Neupane *et al.*, *Phys. Rev. B* **83**, 094522 (2011).
  - [32] A. D. Christianson *et al.*, *Phys. Rev. Lett.* **103**, 087002 (2009).
  - [33] F. L. Ning *et al.*, *Phys. Rev. Lett.* **104**, 037001 (2010).
  - [34] D. K. Pratt *et al.*, *Phys. Rev. Lett.* **106**, 257001 (2011).
  - [35] H. Hodovanets *et al.*, to be submitted to PRB.
  - [36] E. D. Mun, *et al.*, *Phys. Rev. B* **80**, 054517 (2009).
  - [37] Y. Ran *et al.*, *Phys. Rev. B* **79**, 014505 (2009).
  - [38] P. Richard *et al.*, *Phys. Rev. Lett.* **104**, 137001 (2010).
  - [39] S. Arsenijević *et al.*, *Phys. Rev. B* **84**, 075148 (2011).
  - [40] T. Morinari *et al.*, *Phys. Rev. Lett.* **105**, 037203 (2010).
  - [41] L. Fang *et al.*, *Phys. Rev. B* **80**, 140508 (2009).
  - [42] N. Doiron-Leyraud, *Phys. Rev. B* **80**, 214531 (2009).
  - [43] J. Custers *et al.*, *Nature* **424**, 524 (2003).
  - [44] S. Hartmann *et al.*, *Phys. Rev. Lett.* **104**, 096401 (2010).
  - [45] N. Ni *et al.*, *Phys. Rev. Lett.* **78**, 214515 (2008).
  - [46] J. H. Chu *et al.*, *Phys. Rev. B* **79**, 014506 (2009).
  - [47] D. K. Pratt *et al.*, *Phys. Rev. Lett.* **103**, 087001 (2009).
  - [48] R. M. Fernandes *et al.*, *Phys. Rev. Lett.* **105**, 157003 (2010).
  - [49] R. A. Borzi *et al.*, *Science* **315**, 214 (2007).
  - [50] Y. Wang *et al.*, *Nature* **423**, 425 (2003).
  - [51] K. Takada *et al.*, *Nature* **422**, 53 (2003).
  - [52] B. Fisher *et al.*, *J. Phys. Condens. Matter* **15**, L571 (2003).
  - [53] V. Hinkov *et al.*, *Science* **319**, 597 (2008).
  - [54] F. Laliberté *et al.*, *Nature Commun.* **2**, 432 (2011).
  - [55] O. R. Jaramillo *et al.*, *Proc. Natl. Acad. Sci.* **107**, 13631 (2010).
  - [56] E. Fawcett *et al.*, *Rev. Mod. Phys.* **66**, 25 (1994).
  - [57] S. L. Bud'ko, N. Ni and P. C. Canfield, *Phys. Rev. B* **79**, 220516 (2009).
  - [58] N. Tsyrlin *et al.*, arXiv:1203.4974v1 (2012).
  - [59] J.-P. Castellan *et al.*, *Phys. Rev. Lett.* **107**, 177003 (2011).
  - [60] M. Matusiak *et al.*, *Phys. Rev. B* **83**, 224505 (2011).